ISSN 0036-0295, Russian Metallurgy (Metally), Vol. 2019, No. 4, pp. 315–325. © Pleiades Publishing, Ltd., 2019.
Russian Text © The Author(s), 2018, published in Deformatsiya i Razrushenie Materialov, 2018, No. 9, pp. 23–32.

STRUCTURE AND PROPERTIES OF THE DEFORMED STATE

Effect of Cold Rolling and Subsequent Annealing on the Microstructure and the Microtexture of Austenitic Corrosion-Resistant Steels

M. V. Odnobokova[a], * and A. N. Belyakov[a]

[a] *Belgorod State University, Belgorod, 308015 Russia*

**e-mail: odnobokova@bsu.edu.ru*

Received March 15, 2018; revised May 16, 2018; accepted May 21, 2018

Abstract—The deformation mechanisms that occur during cold rolling of austenitic corrosion-resistant steels and the mechanisms of forming of an ultrafine-grained structure in them during subsequent annealing are studied. The structure forming mechanisms are found to be related to the microtexture evolution.

Keywords: austenitic corrosion-resistant steel, rolling, deformation martensite, annealing, recrystallization, microtexture

DOI: 10.1134/S003602951904027X

INTRODUCTION

Austenitic corrosion-resistant chromium–nickel steels are among the most required structural materials, which are widely used in various fields of industry [1]. The technology of manufacturing semiproducts from these steels usually involves cold rolling and subsequent annealing [2–4]. The advantage of applying cold rolling to austenitic corrosion-resistant steels, which have a low energy of stacking fault and, as a result, a high rate of the structural fragmentation is a substantial increase in their strength [5–11]. The yield strength of these steels subjected to cold rolling can be higher than 2000 MPa [8–10]. On the other hand, high degrees of cold deformation lead to deterioration of the plasticity: the relative elongation decreases to several percent [7–11]. This disadvantage restricts the use of cold-rolled austenitic corrosion-resistant steels as semiproducts for subsequent operations of cold shaping.

The common approach to the recovery of plasticity and austenite structure in cold-rolled austenitic corrosion-resistant steels is subsequent heat treatment at temperatures lower than the discontinuous recrystallization temperature.

Such a combination of cold rolling and heat treatment should promote the reverse phase transformation without substantial coarsening of structural elements, which enables one to achieve an increased strength of austenitic corrosion-resistant steels with a sufficient resource of plasticity. Thus, an improved combination of the mechanical properties of austenitic corrosion-resistant steels can be obtained by the formation of an ultrafine-grained structure (UFG) [12–14]. An UFG is easily formed in cold-rolled steels upon annealing as a result of the reverse $\alpha' \rightarrow \gamma$ phase transformation with subsequent development of the continuous recrystallization. Unlike discontinuous recrystallization, continuous recrystallization does not contain the stage of nucleating new grains and is developed immediately during heating an UFG obtained as a result of large plastic deformations [15].

Despite numerous studies of austenitic corrosion-resistant steels subjected to cold deformation and subsequent annealing [16–18], the mechanism of forming UFG and the stability of such a structure on annealing are not studied in detail. In addition, the correlation of the mechanisms of structure forming with the evolution of texture remains unclear. This correlation should be studied on the local microtexture formed in one grain or a grain group rather than on the macrotexture [19]. In this connection, the aim of this work is to study the evolution of the microstructure and the microtexture in austenitic corrosion-resistant steels during cold rolling and subsequent annealing.

EXPERIMENTAL

We studied austenitic corrosion-resistant 03Kh19N10 and 03Kh17N12M2 steels (Table 1). The preliminary thermomechanical treatment of these steels consisted in hot forging and annealing at 1100°C with subsequent cooling into water; as a result, initial microstructures were obtained with average grain sizes 24 and 21 μm in the 03Kh19N10 and 03Kh17N12M2 steels, respectively. The rolling of specimens with an initial cross-section of 30 × 30 mm

Table 1. Chemical compositions of the steels, wt %

Steel	Fe	C	Cr	Ni	Mn	Si	Mo	P	S
03Kh19N10	Balance	0.05	18.2	8.8	1.65	0.43	—	0.05	0.04
03Kh17N12M2	Balance	0.04	17.3	10.7	1.70	0.40	2.0	0.04	0.05

was carried out in flat rolls at room temperature to a true strain $e \approx 0.5$, 1, 2, and 3. Steel strips after cold rolling to $e = 3$ were annealed in the temperature range 600–800°C for 1 h in a Nabertherm LT5/12/b180 muffle furnace with subsequent cooling into water.

The microstructure was studied using a Nova Nanosem 450 scanning electron microscope equipped with a detector recording electron back-scatter diffraction (EBSD) patterns. The structural studies were carried out on a transverse cut of rolled specimens along the rolling direction. The results were processed with the TSL OIM Analysis software to built orientation distribution functions (ODFs) to estimate the texture formed after rolling and subsequent annealing.

Table 2. Texture components and texture fibers typical of austenite and martensite

Component	{*hkl*} ⟨*uvw*⟩	Euler angles, deg		
		φ_1	Φ	φ_2
Cube	{001}⟨100⟩	45	0	45
Rotated cube	{001}⟨110⟩	0; 90	0	45
E	{111}⟨110⟩	0; 60	55	45
F	{111}⟨112⟩	30; 90	55	45
I*	{223}⟨110⟩	0	43	45
Goss	{110}⟨001⟩	90	90	45
Rotated Goss	{110}⟨110⟩	0	90	45
Brass	{110}⟨112⟩	55	90	45
A	{110}⟨111⟩	35	90	45
Copper	{112}⟨111⟩	90	35	45
S	{123}⟨634⟩	59	37	63
γ-Fiber	⟨111⟩‖ND			
ζ-Fiber	⟨110⟩‖ND			
α-Fiber	⟨110⟩‖RD			
τ-Fiber	⟨110⟩‖TD			
η-Fiber	⟨001⟩‖ND			

* ND is the normal direction to the rolling plane; RD, the rolling direction; and TD, the transverse direction.

The equilibrium phase composition was calculated using the Thermocalc software and the TCFE7 data base, The volume fraction of deformation martensite (α') was estimated by X-ray diffraction and EBSD and also using a ferritoscope. The grain size was found using microstructure images reconstructed from EBSD data using the random linear-intercept method in the direction perpendicular to the rolling direction (all high-angle boundaries were taken into account). The Vickers microhardness was measured by a 402MVD Instron Wolpert microhardness tester at a load of 3 N.

RESULTS AND DISCUSSION

Early at the stages of cold plastic deformation (to $e = 0.5$) in the 03Kh19N10 and 03Kh17N12M2 steels, grains elongate along the rolling direction and deformation twinning is developed inside grains (Fig. 1). The formation of twin boundaries favors the martensitic $\gamma \rightarrow \alpha'$ transformation. It should be noted that the 03Kh19N10 steel is characterized by faster kinetics of the martensitic transformation; as a result, cold rolling to $e = 0.5$ is sufficient for the formation of a two-phase structure consisting of austenite and martensite grains in the steel (Fig. 1), and the fraction of martensite is about 0.2 (Fig. 2). For the martensitic transformation to be actively developed in the 03Kh17N12M2 steel, higher degrees of plastic deformation are necessary.

Further deformation leads to larger elongation of grains along the rolling direction and the formation of shear microbands, which favor additional fragmentation of initial austenite grains. Shear microbands are preferable places of nucleation of deformation martensite; thus, their appearance favors an increase in the fraction of martensite at intermediate degrees of strain ($e = 1$).

At high degrees of strain, grain elongation forms a wavy microstructure along with the development of shear microbands. So, the microstructure of the 03Kh19N10 steel strongly deformed after rolling to $e = 3$ consists of elongated wavy martensite grains (their fraction is 0.75 (Fig. 2)), which alternate with chains of fine austenite grains. The 03Kh17N12M2 steel structure at $e = 3$ consists of elongated austenite grains separated by nanodimensional deformation martensite grains, whose fraction is 0.25 (Fig. 2). The fraction of deformation martensite in the 03Kh19N10 steel after

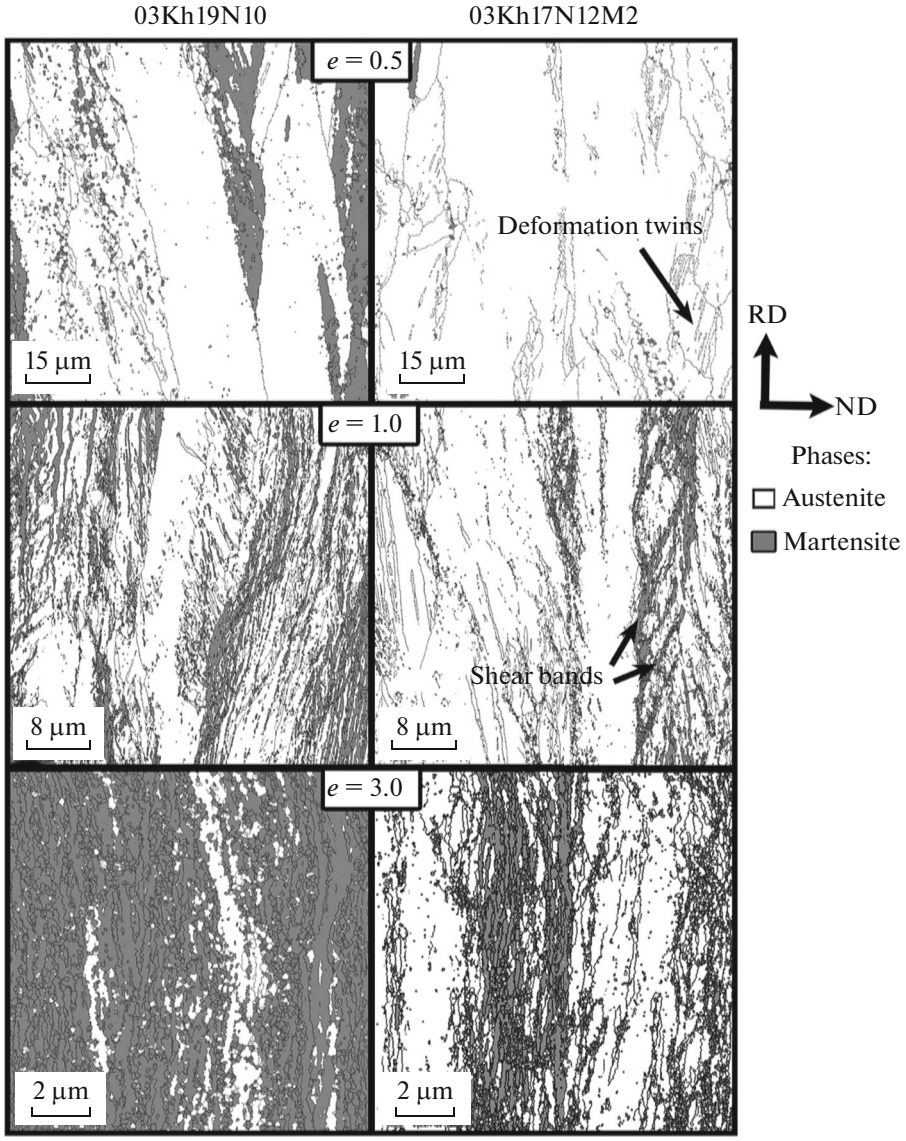

Fig. 1. Microstructures of 03Kh19N10 and 03Kh17N12M2 steels after cold rolling to a true strain $e = 0.5$, 1, and 3. Black lines correspond to high-angle boundaries.

rolling to $e = 3$ approaches the value calculated using the ThermoCalc program; in this case, the fraction of deformation martensite in the 03Kh17N12M2 steel is only 30% of that calculated with the ThermoCalc program.

The microstructure evolution mechanisms in these steels during cold rolling influence the grain boundary misorientation distributions (Fig. 3). After deformation to $e = 0.5$, the misorientation angle distribution of grain boundaries in the 03Kh19N10 steel is characterized by three peaks, which correspond to angles $\theta < 10°$, $\theta \approx 45°$ and 60°. The first peak is related to the formation of low-angle subboundaries during plastic deformation [20]. The second peak corresponding to boundaries with a misorientation of about 45° is due to the martensitic transformation, since the orientation relationships between austenite and martensite in austenite steels are described by the Kurdjumov–Sachs and Nishiyama–Wassermann relationships. According to these relationships, the misorientation between phases γ and α is 42.9° and 46°, respectively [8]. The third peak characterizes the development of deformation twinning, since it is known that the misorientation of a twin boundary in austenite is 60° in the ⟨111⟩ direction.

The misorientation angle distribution of grain boundaries after cold rolling to $e = 0.5$ for the 03Kh17N12M2 steel contains only two peaks, at $\theta < 10°$ and $\theta \approx 60°$. The peak that corresponds to boundaries with $\theta \approx 45°$ appears after rolling to $e = 1$. During

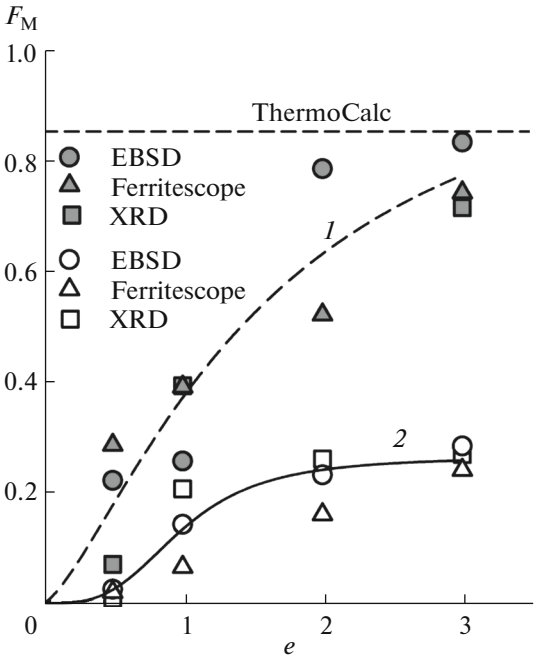

Fig. 2. Strain dependence of the fraction of deformation martensite in (*1*) 03Kh19N10 and (*2*) 03Kh17N12M2 steels.

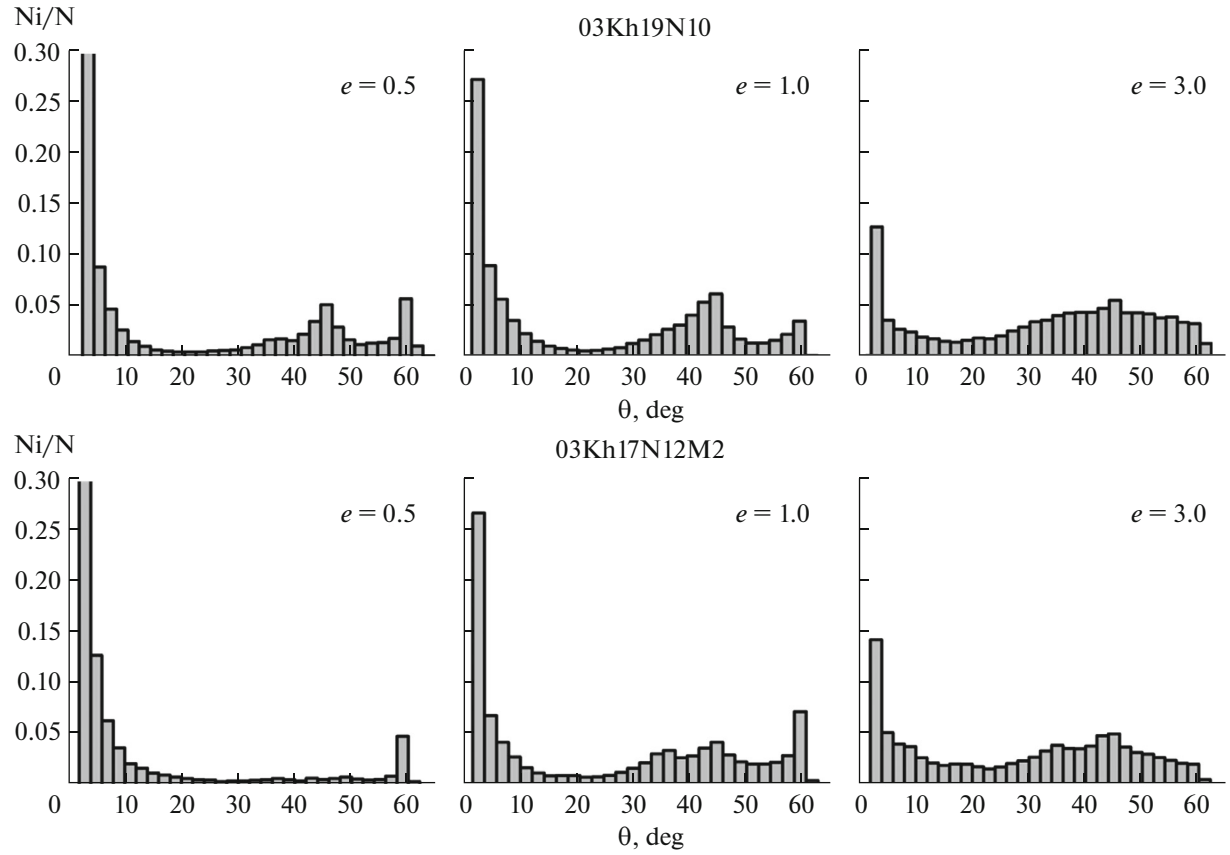

Fig. 3. Distribution of grain boundary misorientations after cold rolling to various degrees of strain for 03Kh19N10 and 03Kh17N12M2 steels.

deformation, the misorientation of deformation subboundaries gradually increases and the fraction of low-angle subboundaries decreases. Deformation twinning characteristic of small degrees of strain does not take place, which is demonstrated by the disappearance of the peak at $\theta \approx 60°$. On the other hand, the deformation martensitic transformation is continuously developed during cold rolling to $e = 3$. As a result, the grain-boundary misorientation in the steels at high degrees of strain has a random distribution with two peaks, which correspond to low-angle misorientations (deformation subboundaries) and the misorientation $\theta \approx 45°$ (result of the martensitic transformation).

The microhardness expectedly correlates to the strain and the grain size. It markedly increases during cold rolling to $e = 0.5$: approximately, from 1360 to 4000 MPa in the 03Kh19N10 steel and from 1440 to 3600 MPa in the 03Kh17N12M2 steel. Then, the rate of strain hardening decreases: the microhardnesses of both steels increases approximately to 5000 MPa as the strain increases to $e = 3$ (Fig. 4). In this case, the 03Kh19N10 steel demonstrates slightly larger strain hardening. The cross-section size of austenite and martensite grains quickly decreases (to 350 and 500 nm in the 03Kh19N10 and 03Kh17N12M2 steels, respectively) during rolling to $e = 1$. As the strain increases further, the rate of grain refining decreases, and the cross-section grain size decreases to 130 nm in both steels as the strain increases to $e = 3$ (Fig. 4). We did not state an explicit dependence between the microhardness and the volume fraction of deformation martensite, which almost linearly increases as the strain increases in the range $0 < e < 2$ (Figs. 2 and 4). This finding is related to fact that these steels contain a low amount of carbon; thus, the martensitic transformation does not make a substantial contribution to the microhardness against the background of strong strain hardening.

After cold rolling to $e = 3$, the austenite texture of both steels is characterized by the predominance of the texture brass component {110}⟨112⟩ (Fig. 5), which is typical of fcc metals with low and moderate stacking fault energies [21, 22]. Its formation is due to the suppression of cross dislocation glide during cold deformation, the development of deformation twinning, and the operation of octahedral slip {111}⟨110⟩. The austenite texture in these steels after cold rolling contains a relatively strong Goss texture component {110}⟨100⟩, which is related to the formation of ultrafine grains in shear bands, along with the brass-type component. The texture of the deformation martensite is characterized by the predominance of strong texture component I* {223}⟨110⟩ along with γ fibers (⟨111⟩‖ND). Similar textures are often observed in bcc metals after high degrees of cold rolling and are usually related to the main slip system {110}⟨111⟩.

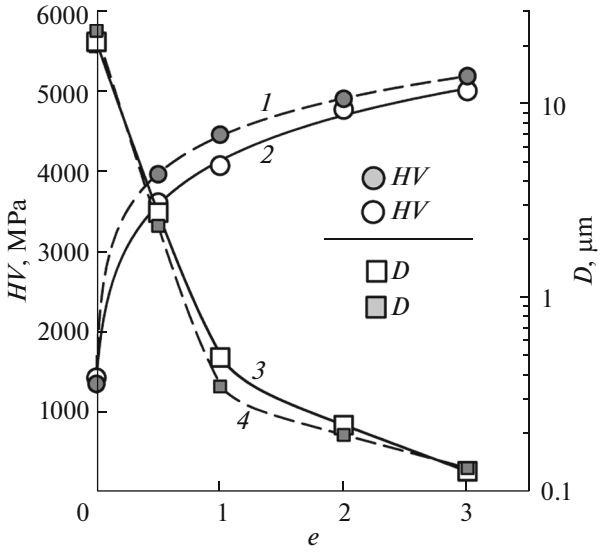

Fig. 4. (*1*, *2*) Microhardness and (*3*, *4*) transverse grain size vs. the strain for (*1*, *4*) 03Kh19N10 and (*2*, *3*) 03Kh17N12M2 steels.

Annealing of the cold-deformed two-phase (γ + α') structure at 600°C leads to the reverse α' → γ phase transformation. It should be noted that deformation martensite is not completely transformed to austenite at an annealing temperature of 600°C. Therefore, the microstructure of both steels is still two-phase: the 03Kh19N10 steel contains approximately 65% austenite and 35% deformation martensite, and the 03Kh17N12M2 steel contains approximately 85% austenite and 15% deformation martensite (Fig. 6). Annealing at 600°C does not lead to substantial changes in the morphology of the grains in the 03Kh17N12M2 steel, and the continuous recrystallization of the 03Kh19N10 steel provides the formation of equiaxed ultrafine grains against the background of the structure strongly extended along the rolling direction.

The conservation of the lamellar grain morphology indicates the reverse α' → γ phase transformation by the shear mechanism [23]. On the other hand, deformation martensite in cold-rolled specimens is completely transformed into austenite on heating to 700°C, which makes continuous collective recrystallization easier. Recrystallized grains form as chains of ultrafine grains at the boundaries of grains strongly extended along the rolling direction and also in shear microbands. As a result of annealing at 700°C, the microstructure of the 03Kh19N10 steel consists of relatively recrystallized grains, while the 03Kh17N12M2 steel microstructure contains unrecrystallized portions. As the annealing temperature increases to 800°C, normal grain growth develops in both steels. It should be noted that the 03Kh17N12M2 steel is char-

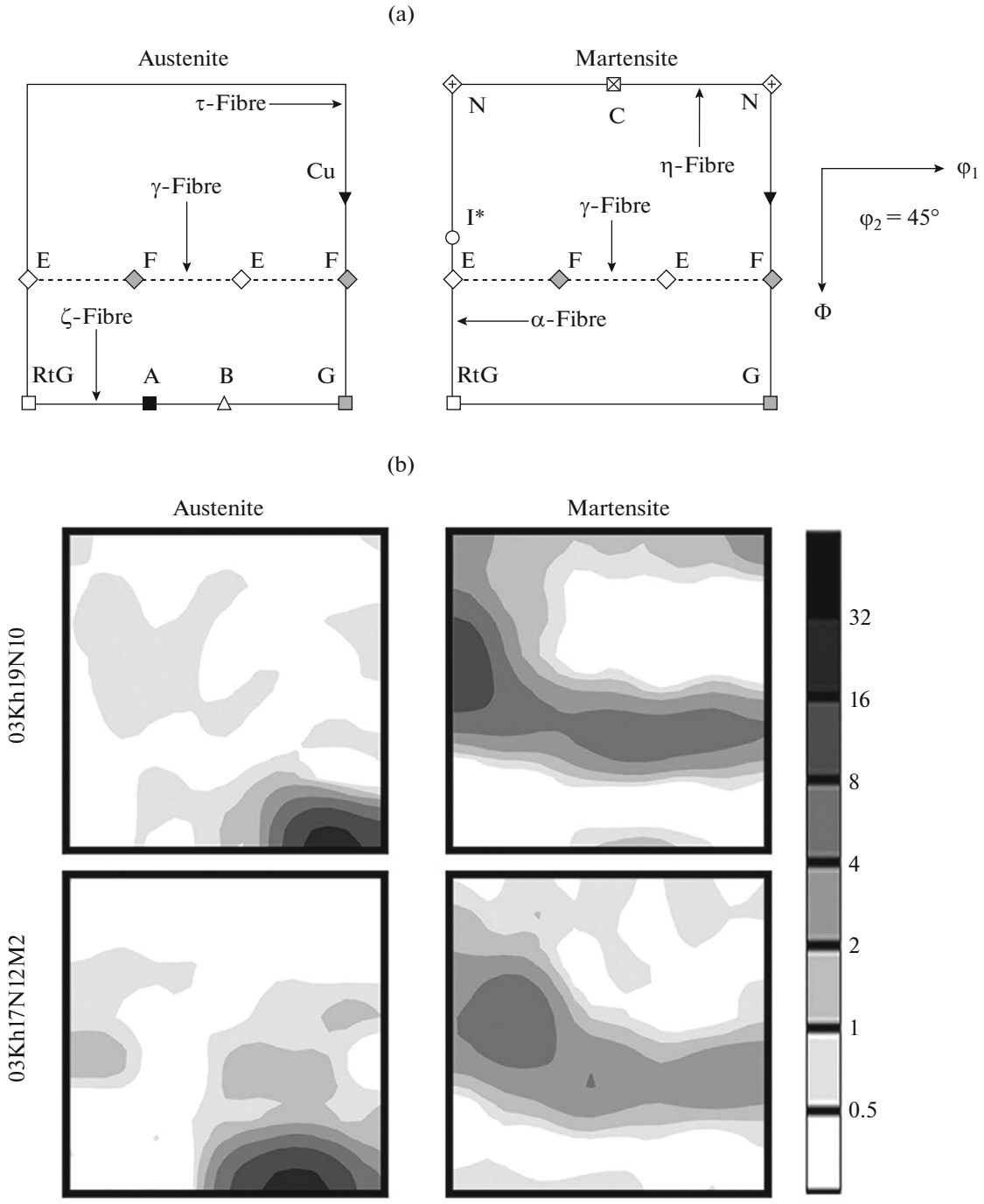

Fig. 5. (a) Schematic representation of the main texture components for austenite and martensite in an ODF section and (b) ODF sections of 03Kh19N10 and 03Kh17N12M2 steels after cold rolling to $e = 3$. The notations of the texture components: C is cube; N, rotated cube; G, Goss texture; RtG, rotated Goss texture; Cu, copper texture; and B, brass texture.

acterized by slower recrystallization kinetics during annealing.

Annealing at 600°C leads to a slight decrease in the hardness (from 5200 to 4570 MPa) of the 03Kh19N10 steel, but in this case the microhardness of the 03Kh17N12M2 steel is changed only slightly to 5000 MPa (Fig. 7). An increase in the annealing temperature from 600 to 800°C leads to a decrease in the microhardness of both steels by a factor of almost two. It should be noted that the 03Kh17N12M2 steel, unlike the 03Kh19N10 steel, is characterized by slower kinetics of disordering during the annealing, which is related to grain growth.

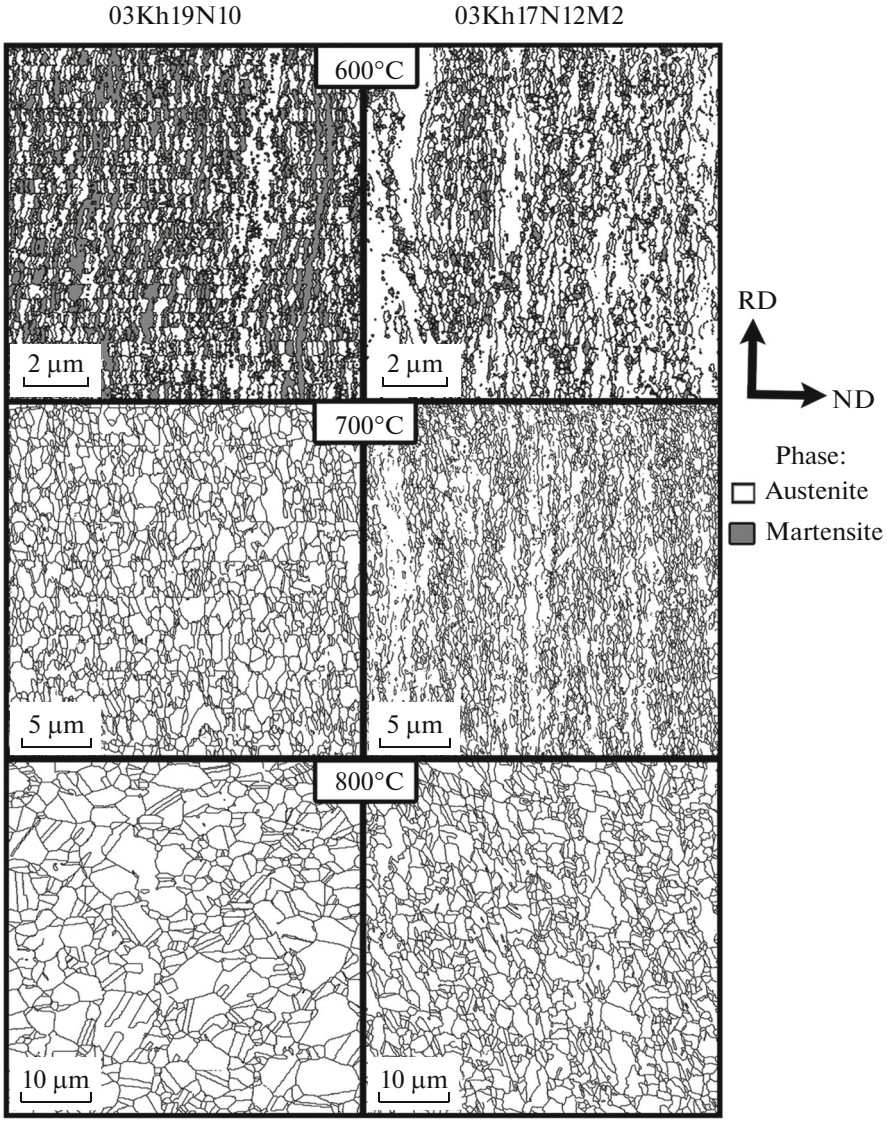

Fig. 6. Microstructures of 03Kh19N10 and 03Kh17N12M2 steels after cold rolling to $e = 3$ and subsequent annealing at 600–800°C. Black lines correspond to high-angle boundaries.

Annealing at 600°C does not lead to substantial grain growth: the grain size is about 180 nm in both steels. Continuous recrystallization during annealing at 700 and 800°C provides fast grain growth. Annealing at 800°C leads to the formation of equiaxed grains, whose cross-section sizes are 1.8 and 1.2 μm for the 03Kh19N10 and 03Kh17N12M2 steels, respectively.

After annealing at 600°C, the cold-rolled steels under study have a two-phase structure with characteristic texture both in austenite and martensite (Fig. 8). In this case, the martensite structure is changed insignificantly and, as a whole, corresponds to the martensite texture after cold rolling (Fig. 5). On the other hand, annealing at 600°C leads to weakening and smearing of the strong brass-type component, which is observed in the austenite structure after cold rolling; as a result, the fractions of the Goss, copper, and S texture components increase (Figs. 7, 8). During annealing at 700°C, the $\alpha' \rightarrow \gamma$ phase transformation is complete; however, it is not accompanied by any marked changes in the final austenite texture after annealing at 700–800°C. Despite a decrease in the fraction of the brass-type component as the annealing temperature increases from 700 to 800°C, the austenite texture annealed at 800°C contains quite strong Goss, copper, and S texture components in addition to the retained brass-type texture component (Figs. 7, 8).

It was shown in [24] that the development of continuous recrystallization in strongly deformed steels is

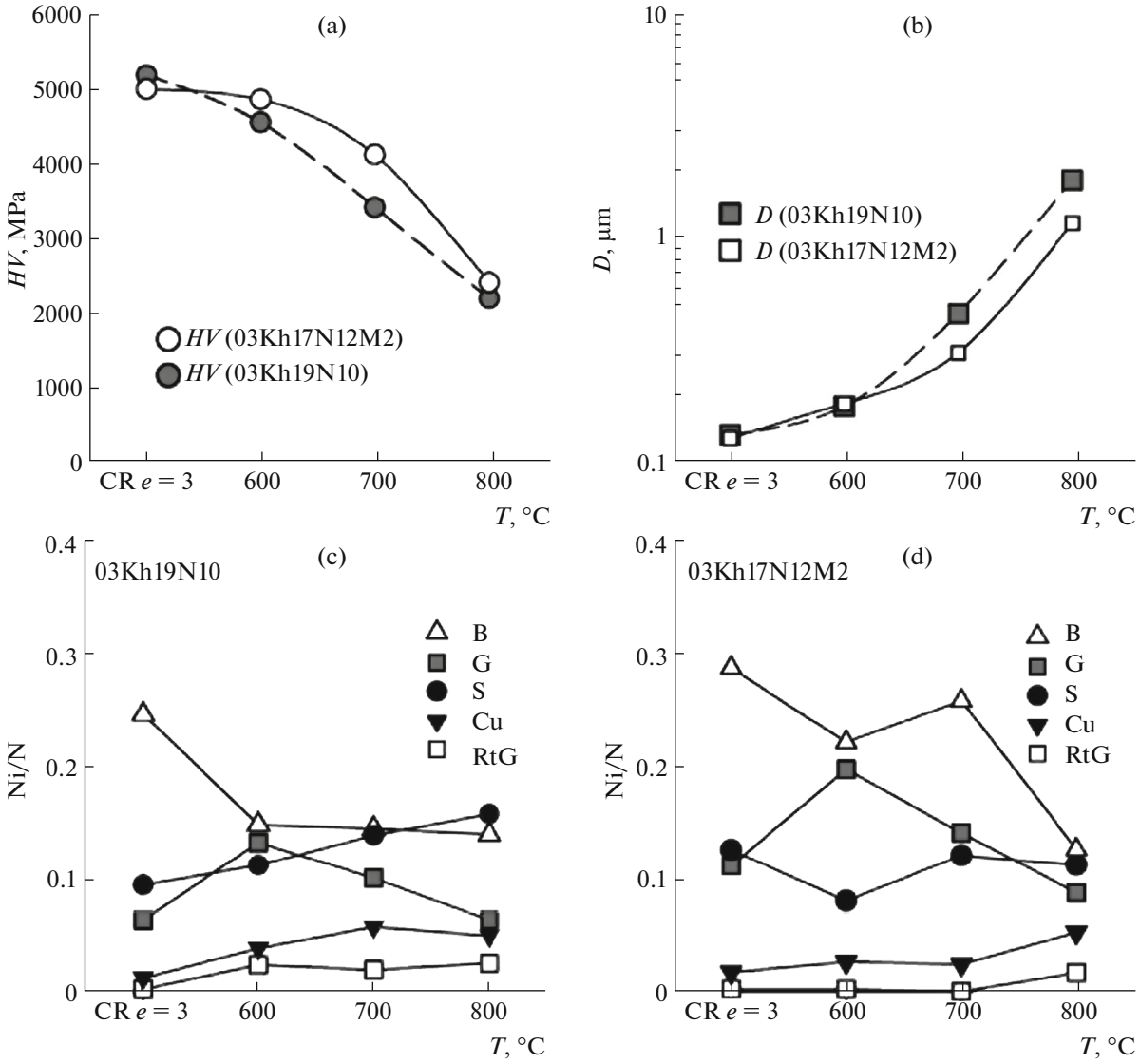

Fig. 7. (a) Microhardness, (b) grain cross-section size, and (c, d) fractions of the main texture components on the annealing temperature for 03Kh19N10 and 03Kh17N12M2 steels; CR is cold rolling.

not accompanied by a significant change in the deformation texture. This fact is related to that the grains formed as a result of continuous recrystallization are essentially grains that formed during previous deformation and grew during subsequent annealing, but normal grain growth should not lead to a change in the texture. The evolution of the microstructure of the cold-rolled 03Kh19N10 and 03Kh17N12M2 steels during annealing is accompanied by smearing of the deformation texture; in this case, the formation of strong new texture components is not observed, which is characteristic of continuous recrystallization (Figs. 5, 8).

Consider the influence of the martensitic transformation on the texture. Since the reverse $\alpha' \rightarrow \gamma$ phase transformation during annealing occurs by the shear mechanism, it proceeds according to the Kurdjumov–Sachs and Nishiyama–Wassermann orientation relationships [25, 26]. The deformation martensite in the cold-rolled a steels is characterized by strong texture component I* (Fig. 5). Figure 8 shows the austenite orientation obtained as a result of the transformation of martensite with orientation {223}⟨110⟩ (I* component) according to the Kurdjumov–Sachs and Nishiyama–Wassermann orientation relationships. The austenite transformed from the deformation martensite with orientation {223}⟨110⟩ can take an orientation close to the Goss, copper, and S texture components (Fig. 9). The S and Goss texture components were observed in cold-rolled austenite. Thus, the difference

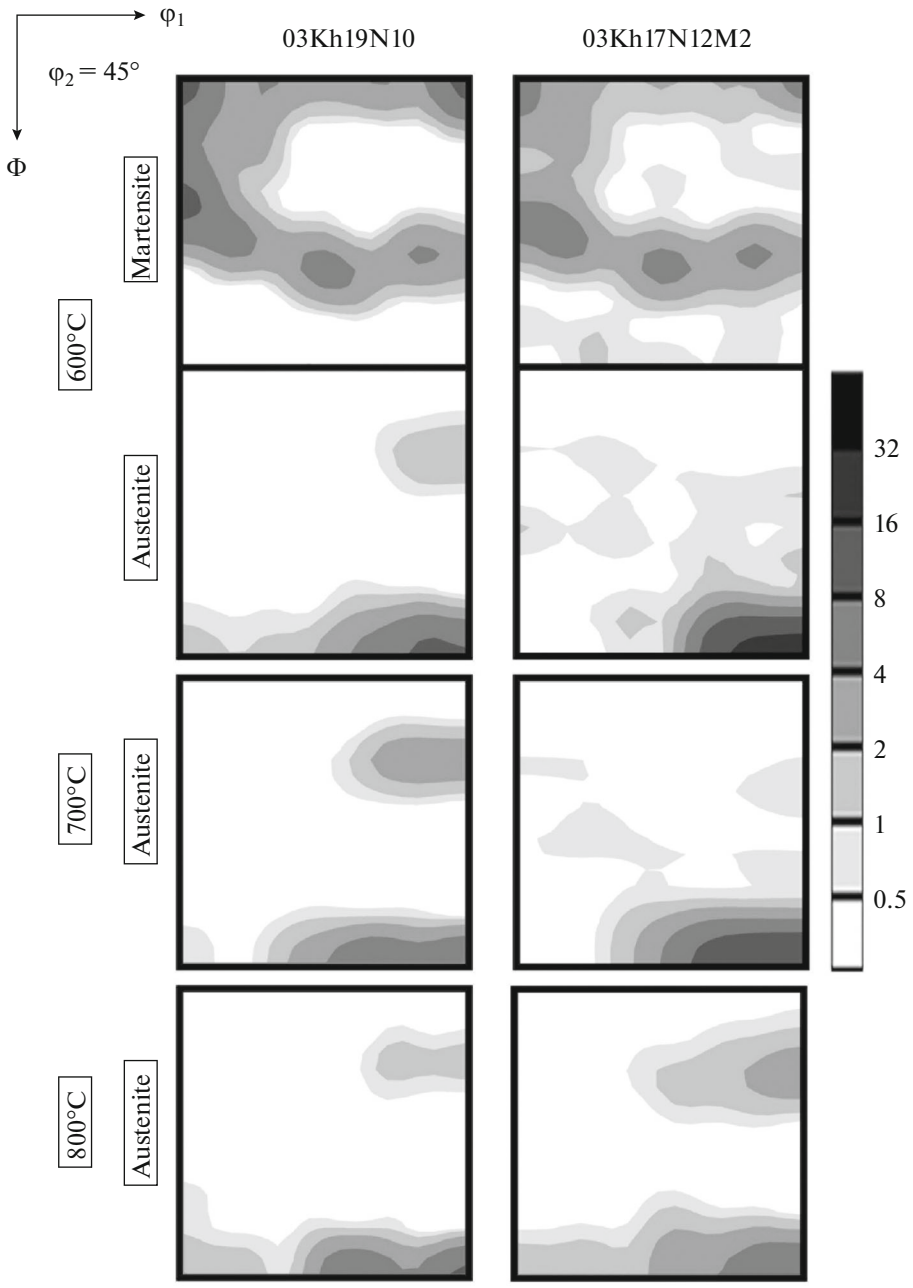

Fig. 8. ODFs of 03Kh19N10 and 03Kh17N12M2 steels after cold rolling to $e = 3$ and subsequent annealing at 600–800°C.

between the cold-rolled texture and the annealing texture consists in the formation of the copper-type texture component, which is actually observed in the textures of the annealed 03Kh19N10 and 03Kh17N12M2 steels.

CONCLUSIONS

The evolution of the structure of austenitic corrosion-resistant steels during cold rolling is characterized by the development of deformation twinning and deformation martensitic transformation, which favor fast grain fragmentation. The structural changes during annealing of the cold-rolled steels are characterized by the reverse phase transformation, which occurs simultaneously with continuous recrystallization and subsequent normal grain growth. The deformation textures degenerate during annealing (although the main texture components are qualitatively unchanged) irrespective of the phase transformation. The texture of the deformation martensite is not changed during annealing and is characterized by

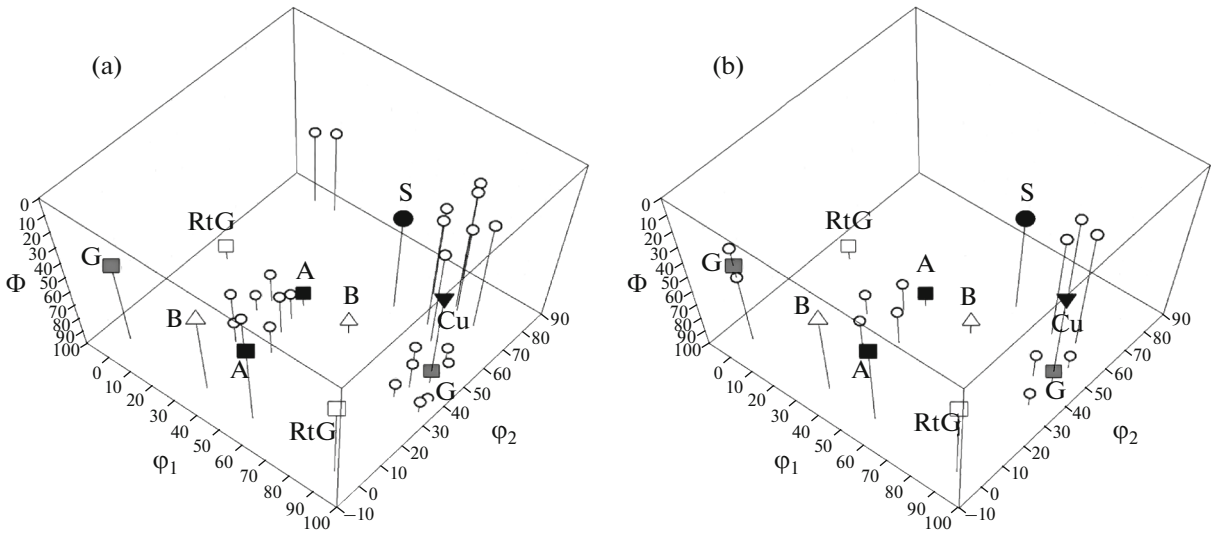

Fig. 9. Austenite orientation obtained as a result of the transformation of martensite with orientation {223}⟨110⟩ according to (a) Kurdjumov–Sachs or (b) Nishiyama–Wassermann orientation relationship.

strong texture component I* and by γ fibers (⟨111⟩‖ND). The fraction of strong brass-type texture component in cold-rolled austenite decreases during annealing, and the fractions of the Goss, copper, and S texture components increase. These texture changes are due to the shear mechanisms of the reverse phase transformation and continuous recrystallization.

ACKNOWLEDGMENTS

Authors are grateful to the personnel of the Joint Research Center of the Belgorod State University for their assistance with the instrumental analysis. The financial support received from the Ministry of Education and Science, Russia, under Grant No. 11.3719.2017/PCh is gratefully acknowledged.

REFERENCES

1. K. H. Lo, C. H. Shek, and J. K. L. Lai, "Recent developments in stainless steel," Mater. Sci. Eng. R **65**, 39–104 (2009).
2. S. G. Chowdhury, S. Das, and P. K. De, "Cold rolling behavior and textural evolution in AISI 316L austenitic stainless steel," Acta Mater. **53**, 3951–3959 (2005).
3. K. Omura, S. Kunioka, and M. Furnkawa, "Product development on market trends of stainless steel and its future prospects," Nippon Steel Techn. Report **99**, 9–19 (2010).
4. I. I. Kosizyna and V. V. Sagaradze, "Phase transformations and the mechanical properties of a stainless steel in a nanostructural state," Izv. Ross. Akad. Nauk, Ser. Fiz. **71** (2), 293–296 (2007).
5. V. V. Sagaradze and A. I. Uvarov, *Hardening and Properties of Austenitic Steels* (RIO UrO RAN, Moscow, 2013).
6. I. Yu. Litovchenko, A. N. Tyumentsev, N. V. Shevchenko, and A. V. Korznikov, "Evolution of structural and phase states at large plastic deformation of an austenitic steel 17Cr–14Ni–2Mo," Phys. Met. Metallogr. **112** (4), 412–423 (2011).
7. Ya. E. Shakhova, Zh. Ch. Yanushkevich, and A. N. Belyakov, "Effect of cold rolling on the structure and mechanical properties of austenitic corrosion–resistant 10Kh18N8D3BR steel," Rus. Met. (Metally), No. 9, 772–779 (2012).
8. Ya. Shakhova, V. Dudko, A. Belyakov, K. Tsuzaki, and R. Kaibyshev, "Effect of large strain cold rolling and subsequent annealing on microstructure and mechanical properties of an austenitic stainless steel," Mater. Sci. Eng. A. **545**, 176–186 (2012).
9. A. Belyakov, A. Kipelova, M. Odnobokova, Ya. Shakhova, and R. Kaibyshev, "Development of ultrafine grained austenitic stainless steels by large strain deformation and annealing," Mater. Sci. Forum **783–786**, 651–656 (2014).
10. A. Belyakov, M. Odnobokova, Ya. Shakhova, and R. Kaibyshev, "Reguliarities of microstructure evolution and strengthening mechanisms of austenitic stainless steels subjected to large strain cold working," Mater. Sci. Forum **879**, 224–229 (2017).
11. M. Odnobokova, A. Belyakov, A. Kipelova, and R. Kaibyshev, "Formation of ultrafinegrained structures in 304L and 316L stainless steels by recrystallization and reverse phase transformation," Mater. Sci. Forum **838–839**, 410–415 (2016).
12. K. Tomimura, S. Takaki, S. Tanimoto, and Y. Tokunaga, "Optimal chemical composition in Fe–Cr–Ni alloys for ultra grain refining by reversion from deformation induced martensite," ISIJ Int. **31**, 721–727 (1991).
13. M. Escandari, A. Kermanpur, and A. Najafizadeh, "Formation of nanocrystalline structure in 301 stainless steel produced by martensite treatment," Metallurg. Mater. Trans. A **40**, 2241–2249 (2009).

14. S. V. Dobatkin, O. V. Rybatchenko, N. A. Enikeev, A. A. Tokar, and M. M. Abramova, "Formation of fully austenitic ultrafine-grained high strength state in metastable Cr–Ni–Ti stainless steel by severe plastic deformation," Mater. Let. **166**, 276–279 (2016).

15. A. Belyakov, T. Sakai, H. Miura, R. Kaibyshev, and K. Tsuzaki, "Continuous recrystallization in austenitic stainless steel after large strain deformation," Acta Mater. **50**, 1547–1557 (2002).

16. D. L. Johannsen, A. Kyrolainen, and P. J. Ferreira, "Influence of annealing treatment on the formation of nano/submicron grain size AISI 301 austenitic stainless steels," Metallurg. Mater. Trans. A **37**, 2325–2338 (2006).

17. C. S. Yoo, Y. M. Park, Y. S. Jung, and Y. K. Lee, "Effect of grain size on transformation induced plasticity in an ultrafine-grained metastable austenitic steel," Scripta mater. **59**, 71–74 (2008).

18. M. Karimi, A. Najafizadeh, A. Kermanpur, and M. Escandari, "Effect of martensite to austenite reversion on the formation of nano/submicron grained AISI 301 stainless steel," Mater. Characteriz. **60**, 1220–1223 (92009).

19. N. Yu. Zolotorevskii and V. V. Rybin, *Fragmentation and Texture Formation upon Deformation of Metallic Materials* (Polytekh. Univer., St. Petersburg, 2014).

20. V. V. Rybin, *Severe Plastic Deformations and Metal fracture* (Metallurgiya, Moscow, 1986).

21. J. Hirsch and K. Lucke, "Mechanism of deformation and development of rolling texture in polycrystalline F.C.C. metals: 1. Description of rolling texture development in homogeneous CuZn alloys," Acta Metallurgica **36**, 2863–2882 (1988).

22. S. S. Gorelik, S. V. Dobatkin, and L. M. Kaputkina, *Recrystallization of Metals and Alloys* (MISiS, Moscow, 2005).

23. M. Odnobokova, M. Tikhonova, A. Belyakov, and R. Kaibyshev, "Development of Σ3n CSL boundaries in austenitic stainless steels subjected to large strain deformation and annealing," J. Mater. Sci. **52**, 4210–4223 (2017).

24. K. Tsuzaki, A. Belyakov, and F. Yin, "Texture invariant annealing in severely deformed steel," Mater. Sci. Forum **558–559**, 101–106 (2007).

25. H. Kitahara, R. Ueji, M. Ueda, N. Tsuji, and Y. Minamino, "Crystallographic analysis of plate martensite in Fe–28.5 at % Ni by FE-SEM/EBSD," Mater. Characteriz. **54**, 378–386 (2005).

26. H. Kitahara, R. Ueji, N. Tsuji, and Y. Minamino, "Crystallographic features of lath martensite in low-carbon steel," Acta Mater. **54**, 1279–1288 (2006).

Translated by Yu. Ryzhkov